

Appraisal of the Cox-Merz rule for well-characterized entangled linear and branched polymers

Frank Snijkers · Dimitris Vlassopoulos

Received: 18 June 2014 / Revised: 14 August 2014 / Accepted: 4 September 2014 / Published online: 16 October 2014
© Springer-Verlag Berlin Heidelberg 2014

Abstract We present a critical assessment of the range of validity of the empirical Cox-Merz rule for a wide range of model entangled polymer samples with a well-defined molecular structure, from linear monodisperse and polydisperse polymers, to branched model polymers (i.e. stars, H-polymers, and combs) and blends of linear polymers of the same chemistry. We focus on melts and concentrated solutions. Overall, we find that the simple empirical rule is obeyed rather well for the investigated cases. As often reported in the literature, relatively small systematic failures occur with the steady viscosity being below the complex one at high rates for most polymers, with linear polydisperse polymers (with a polydispersity index of about 2) being a notable exception. For the latter polymers, the rule is obeyed identically within experimental error. More unusual failures, with the steady shear viscosity being higher than the complex viscosity, are found for branched polymers with more than one branch point. More specifically, these unusual failures are observed at very high branching levels, when the backbone of the polymer is being stretched at low rates due to the motion of the branch points. The extra stress coming for the stretch renders the steady viscosity higher than the complex one. Due to the well-characterized nature of the combs, we can state that failures of the latter type are only apparent when the branches comprise more than 70 % of the molecular structure of the comb. This estimation could serve as a rough guideline in

applications, although it is only a necessary and not sufficient condition for these failures to occur.

Keywords Cox-Merz rule · Shear viscosity · Linear polymer melts · Branched polymer

Introduction

The rheological behavior of polymer melts remains a topic of great scientific and technological interest. The big breakthrough in the understanding of polymer dynamics came with the pioneering works in the 1970s of de Gennes (de Gennes 1971) and Doi and Edwards (Doi and Edwards 1978a; Doi and Edwards 1978b; Doi and Edwards 1978c; Doi and Edwards 1979; Doi and Edwards 1986). The resulting “tube model” in which the description of a single polymer chain diffusing in a tube was postulated to be representative for the whole dynamics of the melt has proven to be extremely successful. The curvilinear diffusion of the chain in the tube was termed “reptation”. Next to reptation, other relaxation mechanisms were later included, mainly contour-length fluctuations (Doi 1983) and thermal constraint release (Marrucci 1985) for linear polymers and, for branched polymers, the coupling of these relaxation mechanisms to different segments of the molecules in a hierarchical fashion (McLeish 1988). Currently, we can state that the modern versions of this popular model, such as the combinatorial hierarchical model of Larson (Larson 2001), branch-on-branch model of Das et al. (Das et al. 2006), and the time-marching algorithm of van Ruymbeke et al. (van Ruymbeke et al. 2006), are able to describe the linear dynamics of a wide variety of polymers, from the simplest linear, monodisperse polymers to more complex linear, polydisperse ones, to branched model polymers (McLeish 2002) and more recently even the most complex commercial samples (Read et al. 2011). Although still

Special issue devoted to novel trends in rheology

F. Snijkers (✉) · D. Vlassopoulos
Foundation for Research and Technology—Hellas (FORTH),
Institute of Electronic Structure and Laser (IESL), Heraklion,
71110 Crete, Greece
e-mail: frank.snijkers@gmail.com

D. Vlassopoulos
Department of Materials Science and Technology, University of
Crete, Heraklion, 71003 Crete, Greece

many issues are outstanding, as e.g. for branched polymers, the exact value for the so-called dynamic dilution exponent α (van Ruymbeke et al. 2012) or the exact amount of branch-point hopping as incorporated via the p^2 parameter (e.g. (McLeish 2002)), and the connection between the polymer synthesis mechanism (Read et al. 2011), the resulting molecular structures, the architectural dispersity in a sample, and the viscoelasticity are still topics of active research; we can state that the (linear) dynamics of polymers is a mature scientific field, and it is relatively well-understood.

Besides linear viscoelasticity, there is great interest in the nonlinear flow behavior of polymers, which is often much more relevant in industry. With the above-mentioned deep understanding of the linear dynamics, nonlinear behavior naturally comes more and more on the forefront of current investigations, with some examples of experimental work on model polymers being studies of the nonlinear shear stress relaxation behavior (Archer and Juliani 2004; Lee et al. 2009; Kapnistos et al. 2009; Kirkwood et al. 2009), the nonlinear start-up shear flow behavior (Menezes and Graessley 1982; Schweizer et al. 2004; Auhl et al. 2008; Liu et al. 2013; Snijkers et al. 2013a; Snijkers et al. 2013b; Snijkers et al. 2013c; Tezel et al. 2009), and the start-up uniaxial extensional flow behavior (Huang et al. 2013; Lentzakis et al. 2013). From an experimental point of view, nonlinear flows are much harder to study compared to the linear dynamics due to a variety of issues with the most important two being (i) the susceptibility of polymer melts to exhibit instabilities in nonlinear deformations (Wang et al. 2011) and (ii) the inherent interest to study well-defined model polymers obtained via controlled polymerization methods for which generally only very small sample quantities are available (Hajichristidis et al. 2000). The small sample quantities pose limits on the applicability of certain techniques. Model polymers are important, as a clear relation between structure and deformation behavior can generally only be established with the help of well-defined molecular structures (McLeish 2002; Graessley 2008). In terms of theory and modeling, the tube model has been extended to describe nonlinear flows as well, although comparisons are generally less successful and the fits not completely parameter free at this time (e.g. (Marrucci 1996; Mead et al. 1998; Mead 2007; Ianniruberto and Marrucci 2002; Ianniruberto and Marrucci 2014; Graham et al. 2003) for linear polymers and e.g. (McLeish and Larson 1998; Das et al. 2014) for branched polymers).

Recently, there have been theoretical efforts to develop alternative frameworks, next to the tube model, that allow one to describe the linear and nonlinear dynamics of polymers. Especially worth mentioning are the so-called “slip-link” models pioneered by Hua and Schieber (Hua and Schieber 1998), which offer comparable predictions to the tube model. Some recent key references on the prediction of the

viscoelasticity and nonlinear flow behavior “using slip-link models are (Doi and Takimoto 2003; Andreev et al. 2014; Yaoita et al. 2012; Masubuchi et al. 2014).

In this paper, we would like to focus very specifically on the validity or possible failure of the well-known Cox-Merz rule (Cox and Merz 1958), which is often used, especially in industry, to predict the hard-to-measure nonlinear shear viscosity from the much more-easily-accessible linear viscoelasticity. The Cox-Merz rule has been examined in the past with commercial linear and branched polymers (see e.g. the discussion in the recent book of Dealy and Larson (Dealy and Larson 2006)), but not with structurally well-defined model polymers. The investigation of the rheological behavior of model polymers with an extremely well-defined molecular structure is important as it allows for an accurate and unambiguous identification of the exact molecular parameters responsible for the observations in general or in this specific case for the validity or failure of the Cox-Merz rule. We present experimental results considering a large variety of different, well-defined polymers (linear monodisperse and polydisperse polymers, star polymers, model branched polymers with more than one branch point, and blends of linear polymers of the same chemistry) and assess the validity of the Cox-Merz rule. Some of the presented nonlinear data were discussed in a different context in earlier works (Snijkers and Vlassopoulos 2011; Snijkers et al. 2013a; Snijkers et al. 2013b; Snijkers et al. 2013c), and some is presented here for the first time. In the next section, we first discuss the empirical Cox-Merz rule in some detail. Subsequently, we discuss the molecular structure of the materials (details of their synthesis can be found elsewhere) and the employed method to investigate their linear and nonlinear rheology. After that, the experimental results are presented to assess the validity of the Cox-Merz rule for a range of different molecular architectures. Finally, we draw conclusions and provide a future perspective for the nonlinear rheology of model polymers.

The Cox-Merz rule: historical perspective

The exact relationship between the complex viscosity η^* and the steady-state viscosity η in the lower limits of frequency and shear rate is well-known and can be expressed as $\lim_{\dot{\gamma} \rightarrow 0} \eta(\dot{\gamma}) = \lim_{\omega \rightarrow 0} \eta^*(\omega)$ (see e.g. (Barnes et al. 1989) and (Macosko 1994)). However, in 1958, Cox and Merz reported that the curve of apparent viscosity η_A as function of shear rate $\dot{\gamma}$, as determined using a capillary rheometer, lay very close to the curve of the complex viscosity η^* versus angular frequency ω over the entire range of frequencies or shear rates. Since that time, the simple “Cox-Merz rule” found widespread use in industry with great success, as linear oscillatory shear measurements are relatively easy to perform even on small sample quantities while the (often more relevant) nonlinear

shear measurements are more difficult and prone to instabilities and slip. As nicely explained in the recent book of Dealy and Larson (Dealy and Larson 2006), the rule has changed face to some extent and the term Cox-Merz rule now generally refers to the (near) equality between the shear rate $\dot{\gamma}$ dependence of the nonlinear steady-state shear viscosity η and the angular frequency ω dependence of the linear complex viscosity η^* , or $\eta(\dot{\gamma}) = \eta^*(\omega)$ for $\dot{\gamma} = \omega$ (see e.g. (Barnes et al. 1989) and (Macosko 1994)). The difference with the originally proposed rule being that the apparent viscosity, as measured in a capillary rheometer, and the steady shear viscosity are not identical due to the inhomogeneous nature of the flow in a capillary rheometer. We further note two alternative views of the Cox-Merz rule that simply differ in the choice of variables and follow directly from the previous one, $\sigma(\dot{\gamma}) = G^*(\omega)$ and $\eta(\sigma) = \eta^*(G^*)$ with σ the (nonlinear) steady-state shear stress and G^* the (linear) complex modulus. They were proposed by Winter (Winter 2009) and can be useful as they provide additional insight into the viscoelasticity and can allow for alternative, more clear comparisons of different materials. In this work, we mainly adhere to the most common interpretation and representation of the rule: $\eta(\dot{\gamma}) = \eta^*(\omega)$, although we do present the data also in the form $\sigma(\dot{\gamma}) = G^*(\omega)$ for two cases.

Since its original publication over half a century ago, the Cox-Merz relationship has been applied to a large variety of systems with varying degrees of success, from polymer melts and solutions to colloidal dispersions (e.g. (Al-Hadithi et al. 1992)). Especially for flexible polymers, the rule seems to work well, and although a clear explanation has now been put forward as to why the rule works for linear polymers (see further), its general applicability remains elusive up to this day. Focusing now on flexible polymers, while linear oscillatory measurements probe the restricted diffusion of the chains (restricted due to entanglements), in nonlinear deformations, additional physics come into play: The polymers can orient and stretch due to the flow; furthermore, in shear flow, the so-called convective constraint release (CCR) of entanglements due to differences in velocity of different sections of the polymer affects the state of stress in the system (Pearson et al. 1991; Marrucci 1996; Ianniruberto and Marrucci 1996). With the additional complexities in nonlinear deformations, there appears to be no reason for a direct connection, let alone equality, between the linear and nonlinear properties apart from their limiting behavior at low frequencies/rates. Hence, it is indeed astonishing that the Cox-Merz rule has any merit at all. Early approaches to explain the rule from Booij et al. (Booij et al. 1983) and Larson (Larson 1985) utilized integral constitutive equations and hence exploited the relationship between the damping and viscosity function. A first truly coherent, molecular explanation for the Cox-Merz rule for linear, monodisperse polymers was given later in 1996 by Marrucci and Ianniruberto and Marrucci; it seems somehow incidental because the CCR mechanism leads to a scaling

of (about) -1 for the steady shear viscosity at high rates, while the entanglement plateau due to rubber-like behavior of the polymers leads to a scaling of (about) -1 as well for the complex viscosity at intermediate to high frequencies. Hence, albeit from a completely different physical origin, incidentally, one arrives at very similar functions for the steady and complex viscosities. More recently, based on the same CCR mechanism but incorporated in a more complete model, Mead (Mead 2011) derived the Cox-Merz rule analytically based on the mixed logical dynamical (MLD) “toy” model for polydisperse linear polymers. The Cox-Merz rule has become such a powerful tool in polymer rheology that when failures are observed, usually with $\eta(\dot{\gamma}) < \eta^*(\omega)$, they are often attributed to instabilities such as secondary flow, slip of the polymer on the walls of the geometry, or edge fracture of the sample rather than a disobedience of this purely empirical rule! Failures with $\eta(\dot{\gamma}) > \eta^*(\omega)$ are much less common but have nevertheless been observed for commercial, branched low-density polyethylene LDPE (Schulken et al. 1980; Booij et al. 1983), and for random branched polystyrenes (Ferri and Lomellini 1999). In the following sections, we will report data for the linear complex and nonlinear steady shear viscosity for model polymers with extremely well-defined molecular architectures: linear monodisperse and polydisperse polymers, model star polymers, model branched polymers with well-defined comb or H-polymer structures, and blends of linear polymers of the same chemistry. The use of model polymers allows us to systematically assess the effects of the molecular architecture on the validity of the Cox-Merz rule.

Materials

We studied different polymers with different molecular structures, as schematically shown in Fig. 1. Two linear, monodisperse polymers of polyisoprene (PI) and polystyrene (PS). The PS was purchased from Polymer Laboratories (UK) and has a weight-averaged molar mass M_w of 182,100 g/mol and a polydispersity index (PDI) of 1.03. Further on, we refer to this polymer as PS182k. The PI was kindly provided by N. Hadjichristidis (University of Athens) and synthesized by high-vacuum anionic polymerization. It has an M_w of 60,000 g/mol and a PDI of 1.10. It has a predominantly 1,4 microstructure ($\sim 83\%$). We labeled this polymer as PI60k. The molecular characteristics are summarized in Table 1, with the reported molar masses being weight averages.

Two linear, polydisperse polymers of PS were obtained from Versalis (Italy). They are commercial polymers used for a large variety of applications, among them are packaging and insulating layers. They are synthesized by radical polymerization. They have a controlled molar mass distribution, and hence, in that sense, we consider them here to be “model” polymers as they allow for an assessment of the effects of

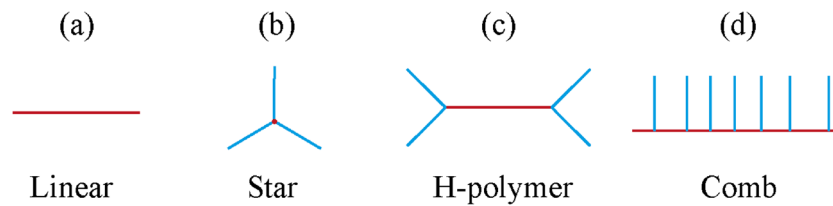


Fig. 1 Different well-defined polymer architectures: **a** linear polymers, **b** low-functionality stars, **c** H-polymers and **d** combs. Note that all polymers of interest here are homopolymers, and hence, the *different colors*

are simply used to discern between different hierarchical levels in the structures (branches versus backbone)

(controlled) polydispersity on the validity of the Cox-Merz rule. The PS124k has an M_w of 124,000 g/mol and a PDI of 1.92, and the PS275k has an M_w of 274,600 g/mol and a PDI of 2.11 (see also Table 1).

Monodisperse, symmetric (i.e. all arms have the same length) star polymers of “low” functionality (Fig. 1c) were synthesized by high-vacuum anionic polymerization as described previously (Snijkers et al. 2013c). They are all PI. The PI4a-56k has four arms with a weight-averaged molar mass of the arms M_{Br} of 56,000 g/mol; the PI8a-56k has eight arms with $M_{Br}=56,000$ g/mol; the PI4a-103k has four arms of 103,000 g/mol. The polydispersity index was in all cases below 1.10. Next to the melts, we also report on data for two solutions of the PI4a-103k in the good solvent squalene (Sigma-Aldrich). They were labeled PI4a-103k86% and PI4a-103k62% with the percentage indicating the volume percentage of polymer in the solution. Their molecular characteristics

are again summarized in Table 1 with q the functionality (i.e. the number of arms) of the star.

The studied H-polymer is a PS; it was synthesized by high-vacuum anionic synthesis by Roovers; and details of its synthesis and viscoelasticity were reported in (Roovers and Toporowski 1981) and (Roovers 1984), respectively. The H-polymer is the most simple and most well-defined molecular structure with more than one branch point (i.e. it has exactly two branches on each end point of the backbone, see Fig. 1c) and with a hierarchy in its relaxation (i.e. first, the branches relax; only after that, the backbone can relax). Its coding is H3A1A, and its molecular details are shown in the last line of Table 1. Columns 3 to 5 in Table 1 contain the weight-averaged molar masses of the complete structure M_{TOT} , the backbone M_{BB} , and an individual branch M_{Br} , respectively. In column 6, q , the average number of branches per backbone, is reported (for the case of an ideal H-polymer, $q=4$). Column 7

Table 1 Molecular characteristics of the different polymers

	Sample	$M_{TOT} 10^{-3}$ [g/mol]	$M_{BB} 10^{-3}$ [g/mol]	$M_{Br} 10^{-3}$ [g/mol]	q [-]	x_c [%]	φ_{BB} [%]	PDI [-]
Linear (PI, PS)	PI60k	60	–	–	–	–	–	1.10
	PS182k	182	–	–	–	–	–	1.03
	PS124k	124	–	–	–	–	–	1.92
	PS275k	275	–	–	–	–	–	2.11
Stars (PI)	PI4a-56k	224	–	56	4	–	–	<1.10
	PI8a-56k	448	–	56	8	–	–	<1.10
	PI4a-103k	412	–	103	4	–	–	<1.10
	PI4a-103k86%	412	–	103	4	–	–	<1.10
	PI4a-103k62%	412	–	103	4	–	–	<1.10
Combs (PI)	PI119k	119	93.5	5.1	5	33	70	1.02
	PI132k	132	85.1	10.2	4.6	67	49	1.03
	PI164k	164	89.3	14.1	5.3	100	37	1.04
	PI254k	254	120.5	18.8	7.1	100	36	1.05
	PI472k40%	472	370	5.8	17.6	29	76	1.02
Combs (PS)	PSc612	477	275	6.5	31	76	55	1.02
	PSc622	626	275	11.7	30	100	41	1.004
	PSc632	918	275	25.7	25	100	28	1.01
	PSc642	1640	275	47	29	100	16	1.003
	PSc652	3120	275	98	29	100	8	1.03
H (PS)	H3A1A	674	123	132	4	0	20	1.004

reports x_c , the fractional length of backbone ends that relax on the timescale of the branches as discussed in the next paragraph. Column 8 reports the relative amount (or volume fraction) of the backbone in the total structure, $\varphi_{BB} = \frac{M_{BB}}{M_{TOT}}$. Note that the simple addition $M_{TOT} = 4M_{Br} + M_{BB}$ is not an identity here due to the addition of reactants to obtain the final H-polymer from the linear backbone and branches and due to experimental errors in the determination of the molar mass as discussed in some detail by Roovers and Toporowski (Roovers and Toporowski 1981). And, the final column contains the PDI as before. A new investigation of the molar mass and its distribution by size-exclusion chromatography (SEC) led to an 8 % lower value of 619,000 g/mol for the weight-averaged molar mass of the total structure.

The model combs (Fig. 1d) are so-called random-branched combs, meaning that the molar masses of backbone and branches are accurately known, as is the average number of branches per backbone but not the exact placement of the branches on the backbone. The combs are either PI or PS. The PS samples were obtained by high-vacuum anionic synthesis (Roovers 1979) and studies of their linear rheology (Roovers and Graessley 1981) and tube-based modeling (Kapnistos et al. 2005) were performed in the past. The PI combs were also synthesized by high-vacuum anionic polymerization (Lee et al. 2009; Kirkwood et al. 2009) and their linear viscoelasticity was investigated for different samples in different publications (Lee et al. 2009; Kirkwood et al. 2009; Snijkers et al. 2013a). An overview of their key structural characteristics can be found in Table 1. The volume fraction of the backbone φ_{BB} is here calculated as $\varphi_{BB} = \frac{M_{BB} - 2x_c M_{BB, end}}{M_{TOT}}$ with x_c the fractional length of backbone ends that relax on the timescale of the branches assuming an equidistant distribution of the branches (Kapnistos et al. 2005; Kirkwood et al. 2009). The PDIs of all the combs are in all cases better than 1.05 as determined by SEC, highlighting the very well-defined nature of the polymers. Also, the newly obtained absolute weight-averaged molar masses of the total structures were always within 10 % of the older values reported in Table 1 (see e.g. (Snijkers et al. 2013a)). Furthermore, these polymers have been investigated with a more advanced chromatography technique, so-called temperature gradient interaction chromatography (TGIC) (Chang 2005), and this technique confirmed the excellent quality, meaning low dispersity of the samples (Snijkers et al. 2013a; Snijkers et al. 2013b). Next to the melts, we also report on data for a solution of PI combs, PI472k40%, in the good solvent squalene (Sigma-Aldrich). Also here, the percentage indicates the volume percentage of polymer in the solution.

With the molecular weights between entanglements M_e for PS and PI being 17,000 g/mol (Roovers and Graessley 1981) and 4,700 g/mol (Kirkwood et al. 2009), respectively, we can

note that all the before-mentioned polymers are in the entangled regime; only for some of the combs, the branches can be relatively small ranging from entanglement densities (in the molten state) of about 0.4 to 6.

Methods

Rheological measurements were performed using the Advanced Rheometric Expansion System (ARES, TA-Instruments, USA) equipped with a convection oven. Measurements were performed in a controlled environment (under nitrogen) with a temperature control of ± 0.1 °C. The linear viscoelastic properties of the polymers were measured using strain-controlled small-amplitude oscillatory measurements using parallel plate geometries made of Invar (a copper-nickel alloy with small thermal expansion coefficient). Measurements were performed at a fixed (small) strain for varying angular frequencies and at different temperatures. Upon changing temperature, appropriate changes in gap spacing were made, thereby taking the thermal expansion of the plates into account. Finally, measurements of the elastic G' and loss G'' moduli as function of angular frequency ω obtained at different temperatures were combined with the help of the RSI Orchestrator software following the well-known time-temperature superposition principle with the horizontal shift factors following the WLF equation and the vertical shift factors calculated from the temperature T [in °C] and the temperature-dependent density ρ as $\frac{\rho(T_{REF}) \cdot (T_{REF} + 273.15)}{\rho(T) \cdot (T + 273.15)}$ (Ferry 1980). The obtained master curves of G' and G'' can then be converted directly in the complex viscosity $\eta^* = \frac{\sqrt{G'^2 + G''^2}}{\omega}$ as function of angular frequency ω .

In one case, for the PI4a-103k, we were not able to reach the terminal flow regime using linear dynamic oscillatory measurements and the accessed frequency range needed to be extended to lower values without using higher temperatures at which the polymer degraded. In that case, long-time constant-stress creep measurements were performed using the stress-controlled Physica MCR 501 rheometer (Anton Paar, Austria) equipped with a homemade aluminum parallel plate geometry with diameter 8 mm as top plate. Temperature control of ± 0.01 °C was achieved with a Peltier system, under nitrogen atmosphere. However, the actual overall temperature control in the sample was not as good (closer to ± 0.1 °C) due to variations in the nitrogen flow in the top part of the Peltier over long times. Linearity of the creep measurements was ensured by performing tests at different stresses. Converting creep compliance versus time curves to the moduli as a function of frequency is well known to be problematic as it is a mathematically ill-conditioned problem. Here, we have followed the the approach of Pasquino et al. (Pasquino et al. 2012).

In addition to linear viscoelasticity, one needs to perform measurements of the nonlinear steady shear viscosity to check

the Cox-Merz rule. We employed a homemade cone-partitioned plate (CPP) geometry (made of stainless steel) on the ARES rheometer following the pioneering designs of Meissner et al. (Meissner et al. 1989) and later works (Schweizer 2002; Schweizer 2003; Schweizer et al. 2004) to measure the nonlinear steady shear flow properties of the polymers in a controlled environment (under nitrogen) and with a temperature control of ± 0.1 °C. The CPP renders measurements of nonlinear shear properties for highly elastic samples more reliable as the influence of edge fracture; the key flow instability for polymers upon entering the nonlinear flow regime is delayed to higher rates and/or higher strains (at a fixed rate). A thorough discussion of our specific setup can be found in (Snijkers and Vlassopoulos 2011). In all reported measurements, the angle of the cone was 0.1 rad; the diameter of the active plate is different in different data sets, either 6 or 8 mm.

Figure 2 shows a typical data set of the start-up shear viscosity η^+ as function of time t for different shear rates $\dot{\gamma}$ as obtained with the CPP at 169.5 °C. The shear rates are indicated in s^{-1} next to the lines. The data shown here are for the H-polymer H3A1A (Table 1). One data set (black lines) was obtained directly at 169.5 °C; the other one (light gray) was obtained at 200 °C and subsequently shifted to 169.5 °C using the horizontal a_T and vertical b_T shift factors from the linear viscoelastic data as indicated in the axes of the graph. The linear viscoelastic (LVE) limiting line is shown in dark gray. It is obtained from the linear viscoelastic data as described previously (Snijkers et al. 2013a). The nonlinear data should follow the LVE limit at low rates and times. Qualitatively, the observations are identical to those reported by Menezes and Graessley (Menezes and Graessley 1982) for solutions of linear and star polymers: The progressive deviation of the transient viscosity data from the LVE envelope as the shear rate increases, marked by a steady-state viscosity value below the LVE one and the occurrence of an overshoot in the time-dependent viscosity

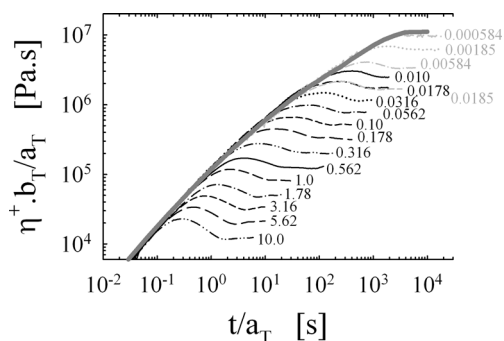


Fig. 2 The start-up shear viscosity η^+ as function of time t for different shear rates for the H3A1A at 169.5 °C. The shear rates are indicated next to the lines in s^{-1} . The light gray data set was obtained at 200 °C and shifted to 169.5 °C using the shift factors from the linear viscoelastic data. The black lines were obtained directly at 169.5 °C. The thick dark gray line is the LVE-limiting line

with increasing shear rate before eventually dropping to its steady-state value. Additionally, at the highest rates, we can observe mild undershoots (i.e. minima in the transient viscosity) before the steady viscosities are reached (see also (Snijkers et al. 2013a)). Note that the nonlinear data does not show any signature of edge fracture for the range of rates and the corresponding time windows as, if the sample was fracturing, the start-up shear viscosity would not reach a steady-state value but would gradually and continuously decrease. Further on in this paper, we only report on the steady-state shear viscosity η_{STEADY} or $\eta(\dot{\gamma})$ as function of shear rate $\dot{\gamma}$ and the complex viscosity η^* as function of angular frequency ω ; discussion of the start-up behavior (i.e. the architectural dependence of the position, breadth, and height of the overshoot) can be found in previous articles (Snijkers and Vlassopoulos 2011; Snijkers et al. 2013a; Snijkers et al. 2013b; Snijkers et al. 2013c). The steady-state shear viscosity is always extracted from the start-up data by taking an average over the steady-state portion of the curves. The standard deviations are also calculated and are in all cases small rendering the error bars obtained in this way smaller than the size of the symbols. Although it is not specifically indicated further on, several nonlinear data sets were often obtained on the same polymer. The different data sets overlap well with errors smaller than the size of the symbols. Hence, since the size of the symbols is a conservative measure for the experimental error, we can state that any visible difference between the linear data (further indicated with lines) and the nonlinear data (indicated with symbols) beyond the size of the symbols is expected to be real and not a result of experimental error. Finally, we can note that we do not further quantify the difference between the linear and nonlinear data, e.g. by calculating the difference or the ratio between the complex viscosity and the steady-state shear viscosity due to the necessity to interpolate the linear complex viscosity data to rates (or frequencies) where nonlinear data is present. Firstly, one has to make a somewhat ambiguous but important choice about how to perform the interpolation. Secondly, the interpolation was found to lead to significant scatter (much larger than the size of the symbols).

Results and discussion

Linear monodisperse and polydisperse polymers

The steady-state shear viscosity η_{STEADY} as function of shear rate $\dot{\gamma}$ is plotted in Fig. 3 (symbols) together with the complex viscosity η^* as function of angular frequency ω (lines) for four different linear polymers. Two of the polymers are monodisperse (green for the PI and blue for the PS) (Snijkers and Vlassopoulos 2011), while the two others are polydisperse PS (black and red). The data on all the PS polymers is either

obtained or shifted to a reference temperature of 170 °C, and the data of the PI is shifted to 20 °C. If the data is shifted, it is done consistently using the shift factors from the linear viscoelastic data both for the linear data and the nonlinear data.

One can observe that all four polymers obey the Cox-Merz rule well (compare lines and symbols of the same color). For the polydisperse polymers (black and red), one cannot discern between the linear and nonlinear data, while for the monodisperse polymers, slight deviations from the rule with $\eta(\dot{\gamma}) < \eta^*(\omega)$ can be observed systematically for both samples at the highest rates. Pattamaprom and Larson (Pattamaprom and Larson 2001) also observed slight deviations of this type for the experimental data on their solutions of monodisperse high molecular weight PS. Their MLD model furthermore supported these deviations. Also, the slip-link model from Hua and Schieber (Hua and Schieber 1998) yields slight discrepancies of this type as reported in (Hua 2000). Similarly, small discrepancies were found for polydisperse PS with PDIs around 1.7 (Ferri and Lomellini 1999), while perfect overlap was found for entangled solutions of monodisperse linear PS but unusual (small) failures with $\eta(\dot{\gamma}) > \eta^*(\omega)$ (at high rates) for PS with a broad molecular weight distribution (Yasuda et al. 1981). The latter observations fit nicely with some of the observations on bidisperse linear polymers (Wen et al. 2004) as discussed in the section on “Bidisperse blends of linear polymers”. Wen et al. (Wen et al. 2004) found excellent agreement of the Cox-Merz rule for their solutions of monodisperse linear PS.

We now discuss the effects of polydispersity on the thinning slopes: The monodisperse polymers are clearly stronger thinning than the polydisperse ones (as expected due to their broader relaxation spectrum), and the slopes of the two monodisperse polymers are identical as are the slopes of the two polydisperse ones which furthermore overlap at high rates. A clear discussion of the shape similarity of the flow curves, and

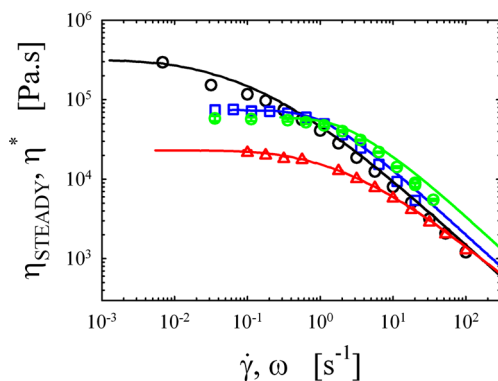


Fig. 3 Steady-state shear viscosity η_{STEADY} (symbols) as function of shear rate $\dot{\gamma}$ and complex viscosity η^* (lines) as function of angular frequency ω for the four linear polymers. Green, blue, red, and black represent the data for the monodisperse PI60k, monodisperse PS182k, polydisperse PS124k, and polydisperse PS275k, respectively. The data of all the PS samples is shown at a chosen temperature of 170 °C, the data for the PI at 20 °C

consequently the possibility to superimpose the curves by appropriate scaling factors for viscosity and shear rate, can be found in Graessley’s recent monograph (Graessley 2008) for linear monodisperse polymers, monodisperse stars, and polydisperse linear polymers (with similar, controlled polydispersity) of varying molecular weight and chemistry.

Model low functionality stars

The steady-state shear viscosity η_{STEADY} as function of shear rate $\dot{\gamma}$ is plotted in Fig. 4 (symbols) together with the complex viscosity η^* as function of angular frequency ω (lines) for a number of different star samples. The data was either obtained directly or shifted to a reference temperature of 20 °C. If the data is shifted, it is done consistently using the shift factors from the linear viscoelastic data both for the linear data and the nonlinear data. A detailed discussion of the nonlinear start-up shear flow and relaxation upon cessation of steady flow behavior of the stars can be found in (Snijkers et al. 2013c). One can observe that the Cox-Merz rule is obeyed rather well in all cases with minor deviations of the type $\eta(\dot{\gamma}) < \eta^*(\omega)$ both for the melts (red, black, and blue) and the solutions (green and gray), as for the linear polymers. Note that, also here, at the highest rates, the data for the different melts overlaps, as for the linear polymers. Menezes and Graessley (Menezes and Graessley 1982) already reported on the start-up shear flow behavior of a well-defined entangled star solution. Because of the occurrence of instabilities, the nonlinear region they accessed was very limited, and hence, their data is not really appropriate to assess the validity of the Cox-Merz rule. On the other hand, due to the special design of their rheometer (Menezes and Graessley 1980), they were able to capture the first normal stress difference reliably. Finally, Tezel et al. (Tezel et al. 2009) studied the nonlinear steady shear viscosity of entangled solutions of star polymers using flow birefringence, and although a direct comparison of linear and nonlinear data was not made, their nonlinear viscosity data is stronger thinning than the data reported in Fig. 4 (as shown in (Snijkers et al. 2013c)) and hence suggest a strong failure of the Cox-Merz rule with $\eta(\dot{\gamma}) < \eta^*(\omega)$.

Model combs

Figure 5 shows the steady (symbols) and complex (lines) viscosities as function of shear rate and angular frequency, respectively, for a whole range of different combs (molecular structures detailed in Table 1). Figure 5a shows the data for the PI combs and PI comb solution at 20 °C; Fig. 5b shows the data for a range of PS combs at 169.5 °C. The data on the PS polymers is either obtained or shifted to the chosen reference temperature of 169.5 °C, and the data of the PI combs and the PI comb solution is either obtained or shifted to 20 °C. If the

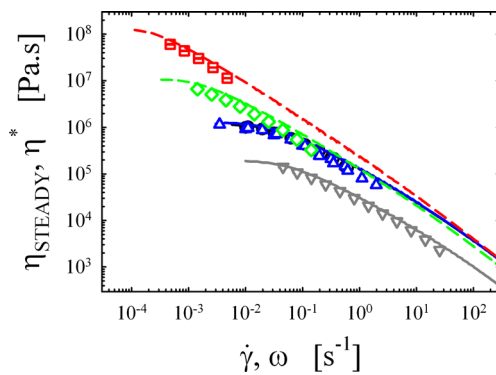


Fig. 4 Steady-state shear viscosity η_{STEADY} (symbols) as function of shear rate $\dot{\gamma}$ and complex viscosity η^* (lines) as function of angular frequency ω for the five different star polymers at a reference temperature of 20 °C. Red, green, gray, black, and blue correspond to the PI4a-103k, PI4a-103k86%, PI4a-103k62%, PI4a-56k, and PI8a-56k, respectively.

data is shifted, it is done consistently using the shift factors from the linear viscoelastic data both for the linear data and the nonlinear data. A detailed discussion of the nonlinear start-up flow and relaxation upon cessation of steady flow behavior for all the PI combs, the PI comb solution, and the PSc612 and PSc622 can be found in (Snijkers et al. 2013a). For the PI combs and the comb solution, one can see in Fig. 5a that the Cox-Merz rule is obeyed very well, with some deviations of the type $\eta(\dot{\gamma}) < \eta^*(\omega)$ at high rates, just like for the linear polymers and stars discussed previously. For the PS combs, the situation is the same for the PSc612 (gray) and PSc622 (green), but for the PSc632, PSc642, and PSc652, one can observe the gradual failure of the Cox-Merz rule in an unusual way with $\eta(\dot{\gamma}) > \eta^*(\omega)$ at intermediate rates. To further clarify, the region of interest is enlarged in Fig. 6a where one can clearly observe the failure (symbols above lines). In Fig. 6b, we further show an alternative view of the data following Winter (Winter 2009) by plotting the steady-state shear stress σ_{STEADY} and complex modulus G^* instead of the steady and complex viscosities. The benefit of this representation is that the scale of the y-axis is about 1.5 decades

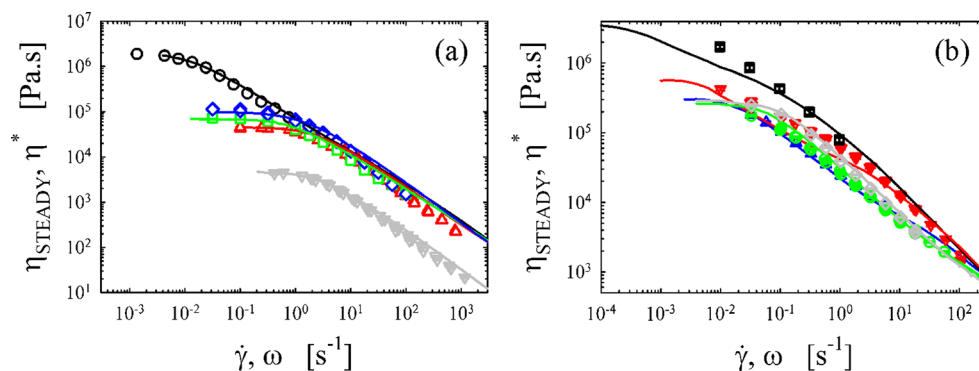


Fig. 5 Steady-state shear viscosity η_{STEADY} (symbols) as function of shear rate $\dot{\gamma}$ and complex viscosity η^* (lines) as function of angular frequency ω for the PI combs and PI comb solution at 20 °C in (a) and for the PS combs at 169.5 °C in (b). In a, the data for the PI254k, PI164k,

smaller, and hence, the differences between linear and nonlinear data are somewhat enlarged. It is further of interest to note that, at the highest rates, the data for the PI combs all overlap very well with each other (apart from the solution), and although much less convincingly, one can also observe this for the PS combs. At the highest rates, the shear flow does not seem to be sensitive to the molecular structure of the polymers (as for the linear polymers and the stars). As can be deduced from Table 1, the key differences in the structures of the PS combs is the increase in the length of the branches when moving through the series from PSc612 to PSc652; the other structural parameters, molar mass of the backbone and number of branches per backbone, remain constant (or nearly so). The failure starts to become visible for the PSc632 as can be observed in Fig. 6a. For the PSc612 and PSc622, the mentioned failure is absent as for the PI combs. Structurally, we can state that the PI combs have fewer and smaller branches as compared to the PS combs for which the failure is observed. When taken the volume fraction of backbone in the structure as structural parameter for the combs, thereby combining the effects of the number of branches and length of the branches in a single parameter (which is surely a very rough approximation), we can state that in terms of volume fraction, the PSc612 and PSc622 fall in the same structural group as the PI combs, while for the other PS combs, the volume fraction of the backbone is significantly lower. In their investigation of the linear viscoelasticity, Roovers and Graessley (Roovers and Graessley 1981) already reported the remarkable transition of the dependence of the recoverable compliance on (in this case) the length of the branches, a dependency that relates to the increasingly strong effects of dynamic dilution on the dynamics of the backbone with increased length of the branches throughout this series of combs. Markedly, also Roovers and Graessley found that the PSc632 was at the point where the transition occurred. Based on the presented data and the range of molecular structures at our disposal, we can argue that volume fractions of branches above 70 % can be reasonably expected to display the unusual failure of

PI132k, PI119k, and PI472k40% are represented by black, blue, green, red and gray, respectively. In b, the data for the PSc612, PSc622, PSc632, PSc642, and PSc652 are represented by gray, green, blue, red, and black, respectively.

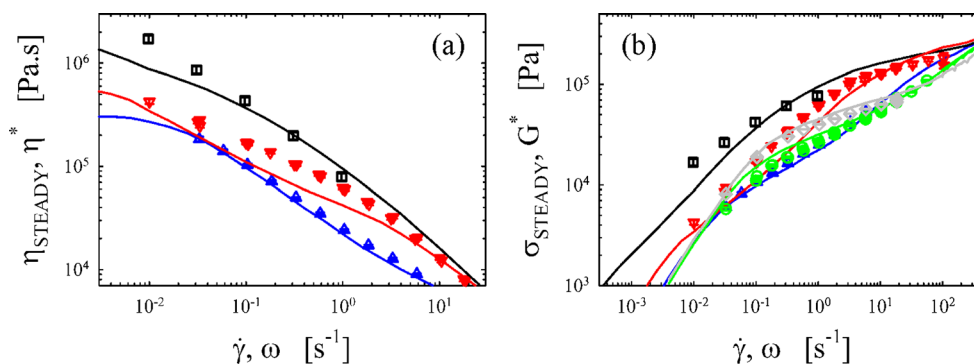


Fig. 6 **a** Zoom-in on the “interesting region” for the data in Fig. 5b. Note the unusual failure of the Cox-Merz rule with $\eta(\dot{\gamma}) > \eta^*(\omega)$. **b** Alternative representation of the data in Fig. 5b: The steady-state shear stress

σ_{STEADY} (symbols) is plotted as function of shear rate $\dot{\gamma}$ and the complex modulus G^* (lines) as function of angular frequency ω . The legends are identical to the one in Fig. 5b

the Cox-Merz rule. Using computer simulations, Snijkers et al. (Snijkers et al. 2013b) found that, due to the molecular structure (i.e. the very long branches), the backbone of the comb with coding PSc642 starts to stretch very early on at rates around its inverse terminal relaxation time; it is most likely the extra stress coming from this “enhanced stretching” which results in the unusual failure of the Cox-Merz rule with higher values for the steady as compared to the complex viscosity.

Model H-polymer

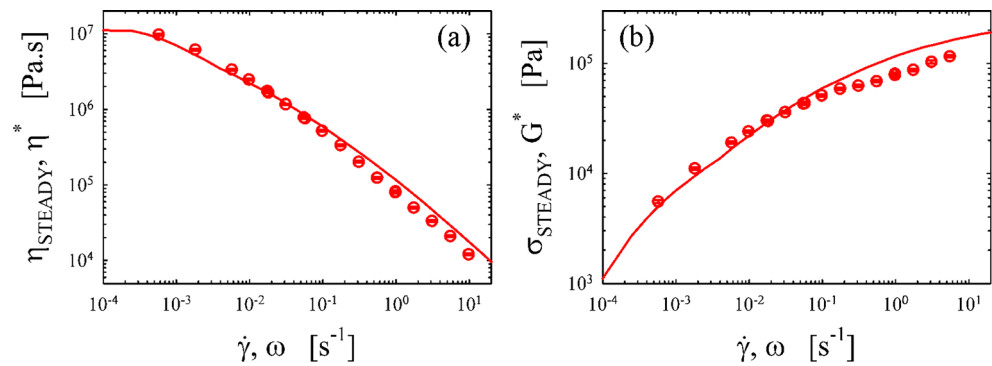
Figure 7a shows the steady (symbols) and complex (lines) viscosities as function of shear rate and angular frequency, respectively, for the H-polymer with coding H3A1A (see Table 1) at a reference temperature of 169.5 °C. The data is either obtained or shifted to 169.5 °C. If the data is shifted, it is done consistently using the shift factors from the linear viscoelastic data both for the linear data and the nonlinear data. In this case, mild failures of the Cox-Merz rule with $\eta(\dot{\gamma}) < \eta^*(\omega)$ at very high rates can be observed, as for the linear polymers, stars, and combs. At intermediate shear rate ranges, one can observe the same unusual failures of the rule with $\eta(\dot{\gamma}) > \eta^*(\omega)$ as for the PS combs with very long branches (PSc632, PSc642, and PSc652). Also here, we provide the reader with the alternative view of the data in Fig. 7b (steady-state shear stress and complex modulus as function of shear rate and angular frequency, respectively, as in Fig. 6b) to further clarify the difference between the linear and nonlinear data. In terms of the before-mentioned structural parameter, the volume fraction of backbone in the structure φ_{BB} , we can note that the value for the H-polymer falls between those of the PSc632 and PSc642 (see Table 1), while the magnitude of the failure of the Cox-Merz rule is less severe for the H3A1A as compared to the PSc642. Most likely, the explanation can be found in the number of section of the backbone. As shown in (Snijkers et al. 2013b), the extra stress coming from the stretch of the backbone increases with the number of segments of the backbone; for the H-polymer, there is only one, while for the PSc642, there are (q-1) or 28 (on average). The same idea

concerning the importance of the number of segments was found to be valid for the behavior of model combs in uniaxial extensional flow by Lentzakis et al. (Lentzakis et al. 2013) as also strain hardening is a result of the stretch of the inner segments of the backbone. This of course also implies that our key structural parameter, φ_{BB} , to classify the behavior of the polymers, is at best an approximation. An assessment of the importance of the separate effects of the number of branches and the length of the branches is at this moment not possible as a larger library of well-defined model branched polymers is currently unavailable.

Bidisperse blends of linear polymers

The interesting case of blends of polymers with the same chemistry but different molecular architecture is an obvious extension. As of yet, we did not investigate any of these situations. There are some earlier works in the literature which address the situation for the Cox-Merz rule for the simplest case of bidisperse blends of two linear monodisperse polymers of the same chemistry, usually in solution (Pattamaprom and Larson 2001; Wen et al. 2004). Studies of this type can be viewed as investigations of the effects of polydispersity (as discussed in relation to the linear polymers), but bidisperse blends are specific from several respects. They are structurally well defined compared to polydisperse polymers. A better structural understanding is convenient, especially when one attempts to model the data. Often, bidisperse blends display phenomena that are qualitatively different from observations on polydisperse polymers. An interesting example is the observations of the double overshoot in start-up shear flow (Osaki et al. 2000). Effects such as the latter are not observed in polydisperse samples because the continuous molecular weight distribution smears out the nonlinearities of individual components over a broad region. Bidispersity hence deserves separate attention and to be complete, we briefly mention the key observations here. Pattamaprom and Larson (Pattamaprom and Larson 2001) found that, for their

Fig. 7 Steady-state shear viscosity η_{STEADY} (symbols) as function of shear rate $\dot{\gamma}$ and complex viscosity η^* (line) as function of angular frequency ω in (a); steady-state shear stress σ_{STEADY} (symbols) as function of shear rate $\dot{\gamma}$ and complex modulus G^* (line) as function of angular frequency ω in (b) for the H-polymer H3A1A at 169.5 °C



bidisperse blends of high molecular weight linear monodisperse polymers of PS (8.43×10^6 g/mol (with PDI 1.14) and 2.89×10^6 g/mol (with PDI 1.09) in 7 vol% solutions in tricresyl phosphate over the full range of compositions), the complex viscosity was generally slightly above the steady viscosity especially at higher rates and at higher concentrations of the long component. As shown in all examples above, this is the common situation. Wen et al. (Wen et al. 2004) observed excellent agreement with the Cox-Merz rule in most cases for a variety of solutions of bidisperse linear PS. In some cases, in a narrow concentration range around 10 % of long chains, they observed a mild upturn of the steady viscosities at the highest rates which resulted in failures of the unusual type with $\eta(\dot{\gamma}) > \eta^*(\omega)$. The phenomenon was attributed to the stretch of the long chains in a sea of shorter chains, not unlike our case for branched polymers where also stretch is at the basis of the reported failure but due to different reasons and over a different range of rates. Note that these experiments might also explain the before-mentioned observations of Yasuda et al. (Yasuda et al. 1981). They found unusual (small) failures with $\eta(\dot{\gamma}) > \eta^*(\omega)$ (at high rates) for PS with a broad molecular weight distribution. The broad distribution in molecular weight can yield a similar effect when an appropriate amount of long chains is stretched. At first glance, the observations of Wen et al. and Pattamaprom and Larson might seem incompatible especially because the samples are comparable in terms of molar masses and difference between the molar masses of the long and short chains. Nevertheless, the latter authors might have missed this slight upturn as they did not investigate a sample in the narrow concentration range around 10 %. We are not aware of any studies of blends of polymer with different architectures in which the Cox-Merz rule is assessed, surely a topic of interest for future work (not only in relation to the Cox-Merz rule).

Conclusions and future perspectives

Although the Cox-Merz rule is purely empirical, it works remarkably well for a large variety of molecular

structures of flexible polymers. If anything, minor deviations of the type $\eta(\dot{\gamma}) < \eta^*(\omega)$ are commonly observed at the highest accessible shear rates, roughly independent of molecular structure. Failures of the type $\eta(\dot{\gamma}) > \eta^*(\omega)$ are much less common. They do exist, and we have shown here that they can be systematically observed at intermediate shear rates for very high levels of branching, as quantified here by the volume fraction of the backbone in the structure. Based on earlier work (Snijkers et al. 2013b), we speculated that the failures relate to the extra stress that arises from the stretching of the backbone in the combs or, more generally, the inner layers of the molecule. The real question is however still opposite: Why does the rule work so well for such a large variety of molecular structures? While the CCR mechanism (Marrucci 1996) offers a clear and concise explanation for monodisperse linear polymers (and, upon extension, also for polydisperse ones (Mead 2012)), for branched polymers and blends, the situation remains elusive although also in their case, CCR can be reasonably expected to be the key mechanism that explains the (approximate) validity. Interesting polymer architectures to challenge the validity of the rule still exist with, e.g. a case of special interest being polymers with a ring architecture. To the best of our knowledge, only linear, complex viscosity data exists for experimentally pure rings (Kapnistos et al. 2008; Pasquino et al. 2013), and nonlinear shear data is completely absent. Also, the validity of the rule for blends of different architectures and the validity of the rule at very high shear rates are as of yet unclear.

The investigation of the rheological behavior of polymers following the outlined approach using structurally well-defined model samples allows for a clear and unambiguous identification of the effects of specific details of the molecular structure of the polymer on the viscoelasticity and flow behavior. As the field of polymer rheology is a mature and well-developed field both experimentally and theoretically, we believe that this approach is currently becoming more and more important and allows for further progress, especially for the further development of existing molecular theories. Currently, there remains much interest in the further elucidation of the effects of molecular architecture of model polymers and polydispersity on the nonlinear shear and extensional flow

behavior with many complementary possibilities for future work, such as further improvement of the techniques for the characterization of nonlinear flow, e.g. the CPP as currently designed in our lab needs further improvements to enable measurements of the first and second normal stress differences following (Schweizer 2002; Schweizer 2003; Schweizer et al. 2004), future investigations into the flow behavior of heavily branched model polymers as the nonlinear rheology becomes more interesting at high branching levels as exemplified here by the failure of the Cox-Merz rule and in Snijkers et al. (Snijkers et al. 2013b) by the occurrence of a double overshoot in start-up shear flow, and investigations of the flow behavior of (miscible) blends of different model architectures.

Acknowledgments We thank J. Roovers, K. Ratkanthwar, and N. Hadjichristidis for generously providing the model branched polymers used in this work. We also thank S. Coppola for generously providing polydisperse linear PS samples. We further thank G. Marrucci, G. Ianniruberto, and R. Pasquino for stimulating discussions. Support from the EU (FP7 ITN DYNACOP, grant 214627 and from the FP7 infrastructure ESML, GA-262348) is gratefully acknowledged.

References

- Al-Hadithi TSR, Barnes HA, Walters K (1992) The relationship between the linear (oscillatory) and nonlinear (steady-state) flow properties of a series of polymer and colloidal systems. *Colloid Polym Sci* 270:40
- Andreev M, Feng H, Yang L, Schieber JD (2014) Universality and speedup in equilibrium and nonlinear rheology predictions of the fixed slip-link model. *J Rheol* 58:723–736
- Archer LA, Juliani A (2004) Linear and nonlinear viscoelasticity of entangled multiarm (Pom-Pom) polymer liquids. *Macromolecules* 37:1076–1088
- Auhl D, Ramirez J, Likhtman AE, Chambon P, Femyhough C (2008) Linear and nonlinear shear flow behavior of monodisperse polyisoprene melts with a large range of molecular weights. *J Rheol* 52:801–835
- Barnes HA, Hutton JF, Walters K (1989) *An introduction to rheology*. Elsevier
- Booij HC, Leblans P, Palmen J, Tiemersma-Thoone G (1983) Nonlinear viscoelasticity and the Cox-Merz relations for polymeric fluids. *J Polym Sci, Polym Phys Ed* 21:1703–1711
- Chang T (2005) Polymer characterization by interaction chromatography. *J Polym Sci B Polym Phys* 43:1591–1607
- Cox WP, Merz EH (1958) Correlation of dynamic and steady flow viscosities. *J Polym Sci* 28:619
- Das C, Inkson NJ, Read DJ, Kelmanson MA, McLeish TCB (2006) Computational linear rheology of general branch-on-branch polymers. *J Rheol* 50:207–234
- Das C, Read DJ, Auhl D, Kapnistos M, den Doelder J, Vittorias I, McLeish TCB (2014) Numerical prediction of nonlinear rheology of branched polymer melts. *J Rheol* 58:737–758
- de Gennes PG (1971) Reptation of a polymer chain in the presence of fixed obstacles. *J Chem Phys* 55:572–579
- Dealy JM, Larson RG (2006) *Structure and rheology of molten polymers*. Publishers, Hanser
- Doi M (1983) Explanation for the 3.4-power law for viscosity of polymeric liquids on the basis of the tube model. *J Polym Sci, Polym Phys Ed* 21:667–684
- Doi M, Edwards SF (1978a) Dynamics of concentrated polymer systems. Part 1—brownian motion in the equilibrium state. *J Chem Soc, Faraday Trans 2(74)*:1789–1801
- Doi M, Edwards SF (1978b) Dynamics of concentrated polymer systems. Part 2—molecular motion under flow 1802-1817. *J Chem Soc, Faraday Trans 2:74*
- Doi M, Edwards SF (1978c) Dynamics of concentrated polymer systems. Part 3—the constitutive equation. *J Chem Soc, Faraday Trans 2(74)*: 1818–1832
- Doi M, Edwards SF (1979) Dynamics of concentrated polymer systems. Part 4—rheological properties. *J Chem Soc, Faraday Trans 2(75)*:38–54
- Doi M, Edwards SF (1986) *The theory of polymer dynamics*. Clarendon Press
- Doi M, Takimoto J (2003) Molecular modelling of entanglement. *Phil Trans R Soc Lond A* 361:641–652
- Ferri D, Lomellini P (1999) Melt rheology of randomly branched polystyrenes. *J Rheol* 43:1355–1372
- Ferry JD (1980) *Viscoelastic properties of polymers*, 3rd edn. Wiley-Interscience, NY
- Graessley WW (2008) *Polymeric liquids & networks: dynamics and rheology*. Taylor & Francis group LLC, NY
- Graham RS, Alexei E, Likhtman AE, Tom CB, McLeish TCB, Milner ST (2003) Microscopic theory of linear, entangled polymer chains under rapid deformation including chain stretch and convective constraint release. *J Rheol* 47:1171–1200
- Hadjichristidis N, Iatrou H, Pispas S, Pitsikalis M (2000) Anionic polymerization: high vacuum techniques. *J Polym Sci A Polym Chem* 38:3211–3234
- Hua CC (2000) Investigations on several empirical rules for entangled polymers based on a self-consistent full-chain reptation theory. *J Chem Phys* 112:8176–8186
- Hua CC, Schieber JD (1998) Segment connectivity, chain-length breathing, segmental stretch, and constraint release in reptation models. I. Theory an single-step strain predictions. *J Chem Phys* 109:10018
- Huang Q, Alvarez NJ, Matsumiya Y, Rasmussen HK, Watanabe H, Hassager O (2013) Extensional rheology of entangled polystyrene solutions suggests importance of nematic interactions. *ACS Macro Lett* 2:741–744
- Ianniruberto G, Marrucci G (1996) On the compatibility of the Cox-Merz rule with the model of Doi and Edwards. *J Non-Newtonian Fluid Mech* 65:241–246
- Ianniruberto G, Marrucci G (2002) A multi-mode CCR model for entangled polymers with chain stretch. *J Non-Newtonian Fluid Mech* 102:383–395
- Ianniruberto G, Marrucci G (2014) Convective constraint release (CCR) revisited. *J Rheol* 58:89–102
- Kapnistos M, Vlassopoulos D, Roovers J, Leal LG (2005) Linear rheology of architecturally complex macromolecules: comb polymers with linear backbones. *Macromolecules* 38:7852–7862
- Kapnistos M, Lang M, Vlassopoulos D, Pyckhout-Hintzen W, Richter D, Cho D, Chang T, Rubinstein M (2008) Unexpected power-law stress relaxation of entangled ring polymers. *Nat Mat* 7:997–1002
- Kapnistos M, Kirkwood KM, Ramirez J, Vlassopoulos D, Leal LG (2009) Nonlinear rheology of model comb polymers. *J Rheol* 53: 1133–1153
- Kirkwood KM, Leal LG, Vlassopoulos D, Driva P, Hadjichristidis N (2009) Stress relaxation of comb polymers with short branches. *Macromolecules* 42:9592–9608
- Larson RG (1985) Constitutive relationships for polymeric materials with power-law distributions of relaxation times. *Rheol Acta* 24:327–334
- Larson RG (2001) Combinatorial rheology of branched polymer melts. *Macromolecules* 34:4556–4571
- Lee JH, Driva P, Hadjichristidis N, Wright PJ, Rucker SP, Lohse DJ (2009) Damping behavior of entangled comb polymers: experiment. *Macromolecules* 42:1392–1399

- Lentzakis H, Vlassopoulos D, Read DJ, Lee H, Chang T, Driva P, Hadjichristidis N (2013) Uniaxial extensional rheology of well-characterized comb polymers. *J Rheol* 57:605–625
- Liu G, Cheng S, Lee H, Ma H, Xu H, Chang T, Quirk RP, Wang S-Q (2013) Strain hardening in startup shear of long-chain branched polymer solutions. *Phys Rev Lett* 111:068302
- Macosko CW (1994) *Rheology: Principles, measurements and applications*. Wiley-VCH
- Marrucci G (1985) Relaxation by reptation and tube enlargement: a model for polydisperse polymers. *J Polym Sci B Polym Phys Ed* 23:159–177
- Marrucci G (1996) Dynamics of entanglements: a nonlinear model consistent with the Cox-Merz rule. *J Non-Newtonian Fluid Mech* 62:279
- Masubuchi Y, Matsumiya Y, Watanabe H, Marrucci G, Ianniruberto G (2014) Primitive chain network simulations for Pom-Pom polymers in uniaxial elongational flows. *Macromolecules*. doi:10.1021/ma500357g
- McLeish TCB (1988) Hierarchical-relaxation in tube models of branched polymers. *Europhys Lett* 6:511–516
- McLeish TCB (2002) Tube theory of entangled polymer dynamics. *Adv Phys* 51:1379–1527
- McLeish TCB, Larson RG (1998) Molecular constitutive equations for a class of branched polymers: the pom-pom polymer. *J Rheol* 42:81
- Mead DW (2007) Development of the “binary interaction” theory for entangled polydisperse linear polymers. *Rheol Acta* 46:369–395
- Mead DW (2012) Analytic derivation of the Cox–Merz rule using the MLD “toy” model for polydisperse linear polymers. *Rheol Acta* 50:837–866, 2011
- Mead DW, Larson RG, Doi M, Mead DW, Larson RG, Doi M (1998) A molecular theory for fast flows of entangled polymers. *Macromolecules* 31:7895–7914
- Meissner J, Garbella RW, Hostettler J (1989) Measuring normal stress differences in polymer melt shear-flow. *J Rheol* 33:843
- Menezes EV, Graessley WW (1980) Study of the nonlinear response of a polymer solution to various uniaxial shear flow histories. *Rheol Acta* 19:38–50
- Menezes EV, Graessley WW (1982) Nonlinear rheological behavior of polymer systems for several shear-flow histories. *J Polym Sci, Polym Phys Ed* 20:1817–1833
- Osaki K, Inoue T, Isomura T (2000) Stress overshoot of polymer solutions at high rates of shear; polystyrene with bimodal molecular weight distribution. *J Polym Sci, Polym Phys Ed* 38:2043–2050
- Pasquino R, Zhang B, Sigel R, Yu H, Öttinger M, Bertran O, Aleman C, Schlüter AD, Vlassopoulos D (2012) Linear viscoelastic response of dendronized polymers. *Macromolecules* 45:8813–8823
- Pasquino R, Vasilakopoulos TC, Jeong YC, Lee H, Rogers S, Sakellariou G, Allgaier J, Takano A, Bras AR, Chang T, Goossen S, Pyckhout-Hintzen W, Wischniewski A, Hadjichristidis N, Richter D, Rubinstein M, Vlassopoulos D (2013) Viscosity of ring polymer melts. *ACS Macro Lett* 2:874–878
- Pattamaprom C, Larson RG (2001) Constraint release effects in monodisperse and bidisperse polystyrenes in fast transient shearing flows. *Macromolecules* 34:5229–5237
- Pearson D, Herbolzheimer E, Grizzuti N, Marrucci G (1991) Transient behavior of entangled polymers at high shear rates. *J Polym Sci B* 29:1589–1597
- Read DJ, Auhl D, Das C, den Doelder J, Kapnistos M, Vittorias I, McLeish TCB (2011) Linking models of polymerization and dynamics to predict branched polymer structure and flow. *Science* 333:1871–1874
- Roovers J (1979) Synthesis and dilute solution characterization of comb polystyrenes. *Polymer* 20:843–849
- Roovers J (1984) Melt rheology of H-shaped polystyrenes. *Macromolecules* 17:1196
- Roovers J, Graessley WW (1981) Melt rheology of some model comb polystyrenes. *Macromolecules* 14:766–773
- Roovers J, Toporowski PM (1981) Preparation and characterization of H-shaped polystyrenes. *Macromolecules* 14:1174
- Schulken RM, Cox RH, Minnick LA (1980) Dynamic and steady state rheological measurements on polymer melts. *J Appl Polym Sci* 25:1341–1353
- Schweizer T (2002) Measurement of the first and second normal stress differences in a polystyrene melt with a cone and partitioned plate tool. *Rheol Acta* 41:337
- Schweizer T (2003) Comparing cone partitioned plate and cone standard plate shear rheometry of a polystyrene melt. *J Rheol* 47:1071
- Schweizer T, van Meerveld J, Öttinger HC (2004) Nonlinear shear rheology of polystyrene melt with narrow molecular weight distribution—experiment and theory. *J Rheol* 48:1345
- Snijkers F, Vlassopoulos D (2011) Cone-partitioned-plate geometry for the ARES rheometer with temperature control. *J Rheol* 55:1167
- Snijkers F, Vlassopoulos D, Lee H, Yang J, Chang T, Driva P, Hadjichristidis N (2013a) Start-up and relaxation of well-characterized comb polymers in simple shear. *J Rheol* 57:1079–1100
- Snijkers F, Vlassopoulos D, Ianniruberto G, Marrucci G, Lee H, Yang J, Chang T (2013b) Double stress overshoot in start-Up of simple shear flow of entangled comb polymers. *ACS Macro Lett* 2:601–604
- Snijkers F, Ratkhanthwar K, Vlassopoulos D, Hadjichristidis N (2013c) Viscoelasticity, nonlinear shear start-up, and relaxation of entangled star polymers. *Macromolecules* 46:5702–5713
- Tezel AK, Oberhauser JP, Graham RS, Jagannathan K, McLeish TCB, Leal LG (2009) The nonlinear response of entangled star polymers to startup of shear flow. *J Rheol* 53:1193–1214
- van Ruymbeke E, Bailly C, Keunings R, Vlassopoulos D (2006) A general methodology to predict the linear rheology of branched polymers. *Macromolecules* 39:6248–6259
- van Ruymbeke E, Masubuchi Y, Watanabe H (2012) Effective value of the dynamic dilution exponent in bidisperse linear polymers: from 1 to 4/3. *Macromolecules* 45:2085–2098
- Wang S-Q, Ravindranath S, Boukany PE (2011) Homogeneous shear, wall slip, and shear banding of entangled polymeric liquids in simple-shear rheometry: a roadmap of nonlinear rheology. *Macromolecules* 44:183–190
- Wen YH, Lin HC, Li CH, Hua CC (2004) An experimental appraisal of the Cox-Merz rule and Laun’s rule based on bidisperse entangled polystyrene solutions. *Polymer* 45:8551–8559
- Winter HH (2009) Three views of viscoelasticity for Cox-Merz materials. *Rheol Acta* 48:241–243
- Yaoita T, Isaki T, Masubuchi Y, Watanabe H, Ianniruberto G, Marrucci G (2012) Primitive chain network simulation of elongational flows of entangled linear chains: stretch/orientation-induced reduction of monomeric friction. *Macromolecules* 45:2773–2782
- Yasuda K, Armstrong RC, Cohen RE (1981) Shear flow properties of concentrated solutions of linear and star branched polystyrenes. *Rheol Acta* 20:163–178